Behaviour of strengthened timber beams using near surface mounted Basalt Fibre Reinforced Polymer (BFRP) rebars

Gand, A., Yeboah, D., Khorami, M., Olubanwo, A. & Lumor, R.

DOI 10.5267/j.esm.2018.7.001
ISSN 2291-8752
ESSN 2291-8744

Publisher: Growing Science

Engineering Solid Mechanics 6 (2018) 341-352

Contents lists available at GrowingScience

Engineering Solid Mechanics

homepage: www.GrowingScience.com/esm

Behaviour of strengthened timber beams using near surface mounted Basalt Fibre Reinforced Polymer (BFRP) rebars

Alfred Kofi Gand[a*], David Yeboah[b], Morteza Khorami[a], Adegoke Omotayo Olubanwo[a] and Richard Lumor[c]

[a]*Sustainable Materials, Structures and Geotechnics Research Group, School of Energy, Construction and Environment, Coventry University, Coventry, West Midlands, UK*
[b]*Independent Research Consultant, UK*
[c]*School of Applied Sciences, Department of Civil Engineering, Central University College, Accra, Ghana*

ARTICLEINFO

Article history:
Received 10 March, 2018
Accepted 5 July 2018
Available online
5 July 2018

Keywords:
Bonded-in rods
Basalt FRP rebars
NSM-FRP
Fibre reinforced polymer
Reinforced timber
Timber strengthening

ABSTRACT

Reinforcement of structural timber members with fibre reinforced polymer (FRP) rods offers merits over that of the conventional steel type. In recent times, near surface mounted (NSM) FRP reinforcement with timber has emerged as a promising alternative for reinforcing timber structures in both flexural and shear loading configurations. Previous investigations have shown that NSM FRP reinforcement technique has higher bond performance than externally bonded equivalents because it (NSM FRP technique) is able to utilise the full capacity of the FRP materials. In spite of these merits, the investigations and the use of this innovative technique are limited. In this paper, an experiment was conducted to investigate the bond characteristics and performance of NSM basalt FRP reinforcement with solid timber structures. In order to predict the performance of the reinforced beam structures, unreinforced control timber members of the same timber characteristics were tested. The results showed that the average bond capacity of the NSM FRP reinforced members was 16% higher than the corresponding unreinforced beams.

1. Introduction

Over the past two decades, fibre reinforced polymers (FRPs) have been used as reinforcement in the strengthening of structural timber (Hollaway & Teng, 2008). The reinforcement of timber with the FRPs and adhesives provides the potential for engineering design and construction. It has been reported by Dempsey and Scott (2006) that adhesive bonding is the best technique for transfer of stresses between the FRPs and the timber. This is because, for adhesive bonding, stress concentration which accompanies mechanical fasteners (such as nails, screws and dowels) is eliminated. Moreover, in adhesive bonding, stresses are uniformly distributed resulting in improved composite interaction between the host timber and the adherents (Adams, 2005). Glass fibre reinforced polymer (GFRP) plastics are considered the most widely used (type of FRP) due to their relative cost efficiency and superior mechanical properties, compared to the aramid and carbon fibres (Bank, 2006). A relatively newer type of FRP is basalt fibre reinforced polymer rods (BFRP). Basalt (also known as solidified

* Corresponding author.
E-mail addresses: a.gand@coventry.ac.uk (A. K. Gand)

doi: 10.5267/j.esm.2018.7.001

volcanic lava) is an extrusive rock which forms when molten lava from deep within the earth upsurges and hardens (Subramanian, 2015). Similar to timber, basalt is classed as a renewable resource and recognised as a complimentary material for sustainability purposes (Zhishen et al., 2012). Experiments of glued-in rods with BFRP have been reported by Yeboah et al. (2013). BFRP rods have also been used as reinforced material in concrete structures, particularly bridge applications (Taylor et al., 2011). In Europe for instance, the first NSM technique with steel reinforced rods for strengthening reinforced concrete elements was reported in 1949. In the last century, more research and applications of the NSM in the strengthening of reinforced concrete elements have been reported. The advantages of FRP over steel as NSM reinforcement are better resistance to corrosion, increased ease and speed of installation due to its lightweight, and a reduced groove size due to the higher tensile strength and better corrosion resistance of FRP. In timber structures, very little research has been conducted using NSM techniques. Silva et al. (2004) have investigated the flexural capacity of NSM FRP structural timber and externally bonded reinforcement (EBR) to determine the shear stress distribution, FRP strain distribution and bond-slip responses. An experimental analysis has been carried out, based on work undertaken by Silva et al. (2004) to determine the maximum composite strength and the maximum composite strain of the timber-FRP beams. It appears that research of NSM with BFRP in timber structures is very limited. Early interventions of using NSM reinforcement was introduced in Europe. This was for the strengthening of reinforced concrete structures. Tests were conducted by Asplund (1949) on concrete beams using NSM steel rebars grout bonded in grooves filled with cement mortar. A study conducted by Morales et al. (2016) involved testing and analysing the effect of using fibreglass and cork plates bonded with epoxy resin and focused on two areas: 1) repairing of beams at end supports (fibreglass) and 2) reinforcement of beams at mid-span, i.e. cork plates. For this study, the timber specimens used in the mid-span test had cross section area of 50 × 50 mm and 900 - 1000 mm long, with varied embedment lengths of between 500 mm and 810 mm. The 1.5 mm thick corks plates were used as backing material whilst the GFRP had two layers bonded with epoxy resin. The study established that the use of GFRP composites was an effective alternative for repairing the beam ends and mid-span. It also highlighted an enhanced load-carrying capacity. A study on the flexural reinforcement of fifteen glulam beams reinforced with BFRP rods, GFRP and CFRP cords was undertaken by Fossetti et al. (2015). The specimen had fabricated groves, measuring 15 × 15 mm and offset of 33 mm from the soffit of the beams. To strengthen the beams, a combination of 2 × 8 mm diameter bars CFRP/GFRP and epoxy resin/melamine glue was adopted. Larger beams were reinforced with 3 × 8 mm diameter bars made up of GFRP cords/BFRP rods and epoxy resin and subjected to four-point loading configuration. The study concluded that the 80 × 130 × 900 mm beams failed by reaching the maximum shear stress of the timber and that the contribution of the FRP rebars resulted in enhanced load capacity and ductility.

Recently, Yousef and Saleh (2010) investigated the flexural behaviour of Yellow Meranti timber beams. The beams, measuring 100 × 200 mm in cross-section and 3000 mm were strengthened with GFRP rebars of varying diameters (96.35 mm, 9.53 mm and 12.7 mm). The bonding agent utilised was a Sika product but no indication of groove size or adhesive bond was mentioned. The study demonstrated an enhanced strength for specimen reinforced with GFRP rebars and that secondary factors such as cracks and knots in the timber resulted in reduced ultimate capacity of some. Also, the stiffness of doubly reinforced strengthened beams was higher compared to singly reinforced equivalents. Lastly, the investigation showed that delamination or debonding of the GFRP rods was not prevalent and that the specimens mainly failed under tension or crushing. In 2009, Alam et al. (2009) considered 36 specimens of fracture beams and repaired them using various reinforcing rebar materials including mild steel, CFRP, GFRP, and a thermoplastic matrix glass fibre reinforced polyurethane (FULCRUM). Grooves were routed in the face of the member and reinforcement added. The CFRP and steel showed the best results for restoring the flexural strength and frequently exceeded its original value. An investigation by Alam et al. (2010) focused on repair of fractured low-grade spruce beams by using steel as a reinforcement material. An enhancement in the strength and stiffness of repaired beam specimen was in the region of up to 114% and 255%, respectively.

Tests on portal joints undertaken by Yeboah et al. (2011) showed that the performance of the joint depended on the strength of timber nearer the tension rods. Yeboah et al. (2012) investigated the enhanced capacity of bonded-in BFRP rod timber beams and affirmed the merits of using BFRP rebars as alternative strengthening material in timber structures. The use of GFRP plates in timber beams have been shown to have significantly improved the ultimate moment capacity of low-grade glulam beams (Raftery & Harte, 2011). The use of carbon fibre reinforced polymer (CFRP) rods in glulam beams has been showed to have enhanced the moment capacity by up to 93% of the equivalent unreinforced control specimen (Micelli et al., 2005; Juvandes et al., 2012). Li et al. (2014) studied natural timber beams strengthened with FRP composite materials by using fungi and insect damaged specimen. Timber hollow sections measuring 150 mm × 150 mm, and spanning 1300 mm, were reinforced with GFRP rods and CFRP sheets in various arrangements, subjected to four-point bending. The study concluded that the ultimate load capacity of the FRP reinforced sections were marginally greater than the controlled section, by between 3.5 and 9.5 percent. Borri et al. (2005) investigated the behaviour of CFRP strengthened timber beams, 200 mm × 200 mm in cross section, and 4000 mm test span. The study reported an enhanced flexural capacity of the strengthened beams bonded with layered CFRP bars by up to 60.3 percent. Post-tensioning of timber beams with basalt FRP tendons has been investigated by McConnell et al. (2014). The study adopted both passive and active reinforcement of glulam timber with bonded and unbonded BFRP tendons, respectively. The result was a more ductile failure mode for passively and actively reinforced glulam timber. Timber specimen actively reinforced using unbonded post-tensioned BFRP tendon had an increased ultimate capacity and stiffness of 28. % and 8.7%, respectively. The bonded equivalent recorded 15.4% and 11.5% in terms of capacity and stiffness, respectively. The stiffness for passively reinforced and bonded BFRP tendon was 15.8%.

Basalt FRP rebars provide merits, comparable to GFRP and CFRP equivalent. CFRP is significantly expensive than GFRP and BFRP. To understand better how the composite structural system, works, it is important for lateral research adopting several timber species and bonding agents. This paper reports experimental observations and results of NSM FRP reinforced structural timber beams bonded with epoxy resins.

2. Methodology

In this section, the materials used for the fabrication of the NSM BFRP reinforced structural timber beams, fabrication of the samples and the test protocols are discussed.

2.1 Materials

The characterisation and properties of timber specimen are outlined. Also presented are the properties of the 2-part thixotropic epoxy resins and 10 mm diameter BFRP rods adopted in the investigation.

2.2 Characterisation of timber specimens

The characterisation specimens used in the experimental testing have been graded as C24 in accordance with BS EN 338-2009, and as stated by the manufacturer. The specimens were fabricated from the beam samples after the flexural tests. The specimens were of nominal cross section dimension, 70 × 70 mm and 150 mm long. The mean density was 536 kg/m^3 and the average moisture content was between 11 - 13%, that highlights service class 2 prior to testing. The characterisation campaign sought to establish the ultimate load, compressive stress, strain and elastic modulus of the timber placed parallel to grain and perpendicular to the grain and was performed in accordance with BS EN 338:2016. A total of ten specimens were fabricated. Presented in Table 1, is the section of the stub specimen. The specimen designation is shown in column 1. Under this column, the reference SPR-$C_{//}$ denotes the stub specimen prepared to be tested under axial compression parallel to the grain. The reference SPP-C_T denotes the stub specimen prepared to be tested under axial compression perpendicular to the grain. Under columns 2, 3 and 4 are the cross-section dimensions and the height. The cross-sectional area

used to determine the compression strength is in column 5. Fig. 1 illustrates the characterisation test setup.

Table 1. Profile of specimen used for the characterisation

Specimen ID	Section Dimensions					
	Measured length (mm)	Measured width (mm)	Measured height (mm)	Cross section area (mm^2)	Compression strength (N/mm^2)	
SPR-C//-1	69.5	69.5	149.0	4830	38.3	
SPR-C//-2	69.0	69.0	149.0	4761	38.7	
SPR-C//-3	70.0	70.0	150.0	4900	28.6	
SPR-C//-4	69.0	69.0	150.0	4761	37.7	
SPR-C//-5	70.0	70.0	150.0	4900	28.1	Avg. = 34.3
SPP-CT-1	70.0	70.0	150.0	4900	9.3	
SPP-CT-2	70.0	70.0	150.0	4900	8.7	
SPP-CT-3	68.0	69.0	150.0	4692	9.9	
SPP-CT-4	69.0	69.0	150.0	4761	14.9	
SPP-CT-5	69.0	69.0	150.0	4761	8.7	Avg. = 10.3

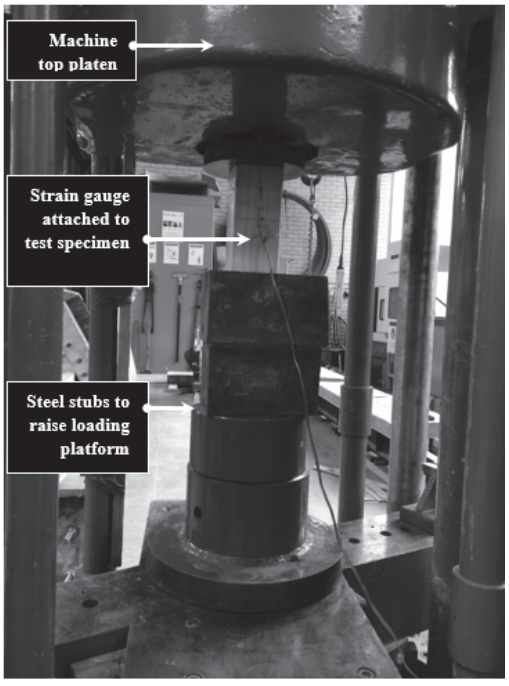

Fig. 1. Characterisation test setup

2.3 Timber specimens

The timber used for the testing was white spruce, which belongs to the Pinus genus. These species of trees are coniferous (evergreen) and are globally one of the most prevalent, although the majority of pine trees are located within the northern hemisphere. To reduce the variability of the host timber samples and to accurately monitor the behaviour of the tested specimens, the timber used for the investigation was delivered from the same batch of sawn lumber. The timber was graded as C24 by the manufacturer in accordance with BS EN 338:2016 and was supplied in lengths of approximately 4000 mm in length with section size of 45 × 145 mm. The mean density was 536 kg/m^3, at approximately 13% moisture content, which highlights pre-test service class 2.

2.4 Basalt fibre reinforced polymer (BFRP) rebars

Basalt fibre reinforced polymer (BFRP) rods, also referred to as rockbars, are low weight, economic, high tensile, corrosion resistant and non-conducting inorganic fibre material. It is pultruded from naturally occurring volcanic basalt rock deposits in a single melt process. The BFRP used in the experimental research were 10 mm diameter reinforcement rods with a coarse-grain sanded finish for improved bonding which were manufactured and supplied by MagmaTech Ltd., UK. The BFRPs polymer matrix consisted of continuous basalt fibre filaments and epoxy resin which comprises both mechanical characteristics of the synergistic materials. Basalt as a composite material was used for the tests due to its exceptional corrosive and heat resistance properties which have gained interest for its benefits in the replacement of asbestos fibres in the construction sector (Urbanski et al., 2013). Basalt rebar is also significantly lighter than conventional steel whilst exhibiting a greater tensile strength. Table 2 defines the material specification of the basalt FRP rebars from the supplier.

Table 2. Basalt FRP material specification

Nominal size (mm)	Ultimate Tensile strength (MPa)	Modulus of elasticity (GPa)
Varied	1000+	>45+

2.5 Adhesive

The NSM FRP reinforcement of timber structures is normally fabricated by adhesive bonding. Several adhesives such as, polyurethanes, epoxies, polyesters, phenolics and aminoplastics have been identified as suitable for bonding of timber with the FRP members (Broughton & Hutchinson, 2003). It has been reported that 2-part epoxy adhesives have generally been found to be most suitable for bonding of timber with FRP due to their superior properties such as good gap-filling properties, being thixotropic and exhibiting low curing shrinkage (Raftery et al., 2009; Davalos et al., 2000; Harvey & Ansell, 2000; Custodio & Broughton, 2008; Burgoyne & Ioannis, 2007). The adhesive used for the present experiment was a 2-part epoxy gap filling (thickness 2 – 12 mm) adhesive, sourced from Rotafix UK, since it was considered the most suitable adhesive for experimental testing as it has been specified for steel and FRP fixings, for applications in timber construction. The adhesive consists of two components, with one of them being the base, containing epoxy resin, including additives. The second component is the curing agent or hardener. They are considered thixotropic, in that, they flow on being sheared but remain static when the shear load is removed. The shear strength of epoxy resin is reported to be two to three times that of timber (Burgoyne & Ioannis, 2007). The manufacturer, Rotafix, stipulates a mix ratio of 1:0.4, that is, one part resin base container (330 g) mixing with one part hardener (145 g). The base and hardener are to be mixed thoroughly until the desired viscosity was sufficient to facilitate the bonding application. The manufacturers curing schedule is in accordance with CEN Standard N20 and the curing properties are noted in Table 3 and Table 4.

Table 3. Rotafix Structural Adhesive curing schedule (Rotafix, UK)

Workability	Gel Point	Peak Exotherm	
		Uninsulated	Insulated
12 hrs at +10ºC	3 Days at + 10ºC	15ºC	20ºC
6 hrs at + 20ºC	2 Days at + 20ºC	30ºC	35ºC
6 hrs at + 30ºC	1 Day at + 30ºC	40ºC	80ºC

Table 4. Rotafix Structural Adhesive full cure properties (+5 Days @ 20°C)

Compressive strength (N/mm^2)	Tensile strength (N/mm^2)	Tensile modulus (GPa)	Flexural strength (N/mm^2)	Bond strength (N/mm^2)	CTE (-60 +40°C) (Deg C-1)
68	38	2.4	70	~6-10	9.2-5

2.6 Fabrication of NSM FRP structural timber beams

Ten NSM FRP timber beams comprising seven reinforced and three controlled or unreinforced beams were studied (Table 5). The experimental tests involved the fabrication of NSM basalt reinforced

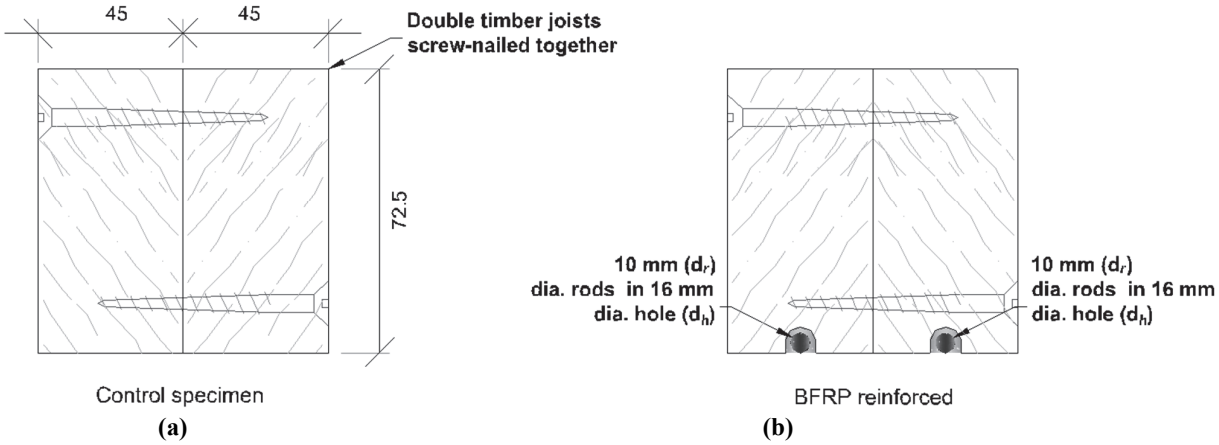

Fig. 2. Section arrangement of unreinforced (a) and reinforced beam (b)

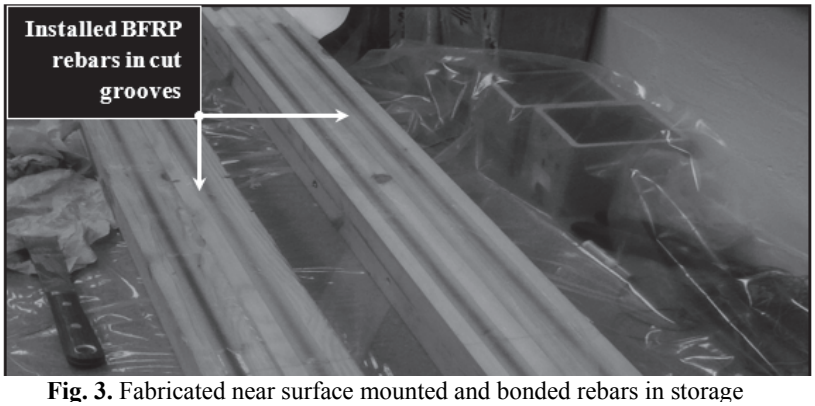

Fig. 3. Fabricated near surface mounted and bonded rebars in storage

timber beams. The unreinforced beams were used as controls to predict the performance of the BFRP reinforced beams. The section arrangement of the strengthened beams comprised circular router cut grooves (resin filled) in the soffit of the beams to facilitate the basalt reinforcements as shown in Fig. 2. The timber beams were manufactured from approximately two 45 × 72.5 mm (breadth × height) cross-section beams. The beams were then screw-nailed together to form a double beam of cross-section 90 × 72.5 mm (breadth × height) and 1200 mm long. The timber beams were manufactured using an NSM technique and were, therefore, fabricated with circular groove cut at the beam soffit. The grooves were cut to a diameter of 16 mm allowing for a 3 mm glue-line (Subramanian et al., 1978). The grooves and the BFRP rods were then coated with a layer of methylated spirit with a clean cloth to decontaminate the surfaces from dust and oils. The 2-part epoxy resin was mixed and then applied to the grooved areas for bonding. The epoxy resin is a slow setting adhesion and therefore allowed 6-hours of workability. The beams were stored in a stable environmental condition of 20°C for a period of 3 days prior to testing to ensure the epoxy was sufficiently cured (see Fig. 3).

Table 5. Experimental test matrix

Specimen ID (No.)	Reinforcement		Cross section area (%)		
	Arrangement		Timber	Rebar	Adhesive
TB-C (3No.)	None	None	1	0	0
TB-BFRP (7No.)	None	BFRP rebars	0.94	0.02	0.04

2.7 Testing protocol

All beams were tested under a three-point bending method as illustrated in Fig. 4. To measure the deflection, a linear variable differential transformer (LVDT) was placed at mid-span. A mechanical digital dial gauge was also positioned at the centre of the beam to endorse the initial LVDT readings. The configuration is shown in Fig. 4. To prevent bearing stresses on the timber beams, a 7 mm thick × 50 mm wide × 125 mm long FRP bearing plate was placed between the loading apparatus and the beams. Steel column supports with 45 mm diameter roller supports were placed at 100 mm from the edge of the beams (length = 1200 mm) as overhang, giving a clear span of 1000 mm and effective span to depth ratio of approximately 14. The loading apparatus consisted of a 60 mm circular roller attached to a hydraulic test machine. A displacement transducer and digital dial gauge were used to measure vertical deflections, at the mid-span. Pinned and roller support conditions were provided. The load was applied vertically downward by means of a Denison test machine with a capacity of 500 kN and controlled hydraulically. Strain distribution was measured using demec strain gauges. The strain gauges were applied to the face of the beams at mid-span above and below the neutral axis. A total of 4 demec linear points were chosen and positioned (see Figs. 4 and 5). The failure mechanisms of the beams during testing were monitored and recorded for analysis.

3. Test Results and Discussion

All the data obtained from the experimental test were analysed and discussed. The strength and stiffness of the BFRP reinforced beams were compared with those of the control beams to determine the performance of the reinforced members. All modes of failure were also evaluated.

3.1 Failure mechanisms of the timber beams

The mode of failure of the unreinforced and reinforced timber beams was observed visually in accordance with EN ISO 10365. Two main failure modes, namely, shear failure and timber splitting, were observed and recorded for the samples.

3.2 Failure mechanisms of the unreinforced members.

Control beam TB-C-01 failed at mid-span due to tensile cracks forming on the timber, shown in Fig. 6. Medium sized knots were detected at the point of rupture which indicated that defects contribute largely to the failure mode of timber beams. Control beam TB-C-02 failed at mid-span where small to medium sized knots were located as a result of cross-grain tension. TB-C-03 also failed in tension due to cracks developing at the soffit of the beam although no knots were detected at mid-span. Horizontal fractures were identified on the timber shortly after the tensile cracking occurred.

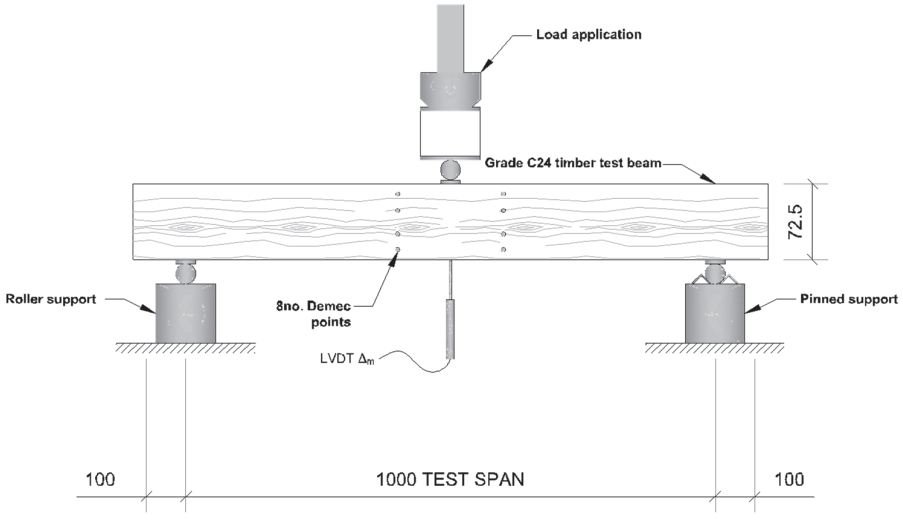

Fig. 4. Schematic test arrangements

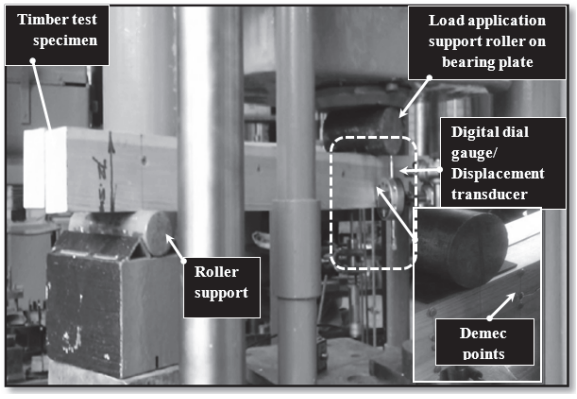

Fig. 5. Experimental test setup

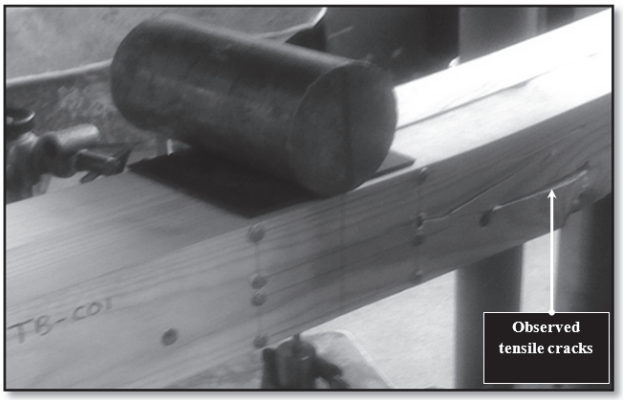

Fig. 6. Formation of tensile cracks at near mid span for specimen TB-C-01

3.3. Failure mechanisms of the NSM BFRP members

Beam TB-BFRP-01 suffered horizontal shear failure of the timber. Minor ruptures were observed at the tension zone and the rebar-adhesive was still intact. This mode of failure occurred due to splits and shakes located at the centre of the cross section shown in Fig. 7. TB-BFRP-01 was, therefore, unable to obtain ultimate load capacity and was consequently the weakest of all the beams tested. Cross-grained tensile failure of the timber occurred in beam TB-BFRP-02. Additionally, severe indentations were detected in the compression zone as the beam reached ultimate load capacity. Similar to TB-BFRP-02, beam TB-BFRP-03 suffered tension and compression failure of the timber. The beam was severely splintered at mid-span which resulted in the adhesive shattering whilst the beam failed. Observation of the adhesive interface showed that the epoxy was still marginally saturated resulting in the debonding of the rebar. Beam TB-BFRP-04 failed in simple tension of the timber. Prior to testing TB-BFRP-04, a large knot was prominent at mid-span. Horizontal shearing and de-bonding of the rebar-adhesive interface occurred shortly after the cracks formed in the tensile zone (see Fig. 8). For beam TB-BFRP-05, the timber suffered severe fractures at mid-span failing in compression and tension. The rebar in specimen TB-BFRP-05 debonded because of the timber splitting (see Fig. 9). Similar to TB-BFRP-05, beam TB-BFRP-06 failed due to splintering at the compression and tension zones. Subsequently, shearing in the timber transpired following the ultimate load capacity. TB-BFRP-07 failed as tensile cross-grained cracks had formed on the timber. Indentations were also detected in the compression zone of TB-BFRP-07. The base of the specimen TB-BFRP-03 suffered moderate splitting at mid-span resulting in the epoxy resin cracking, with the Rockbar remaining unaffected (see Fig. 10).

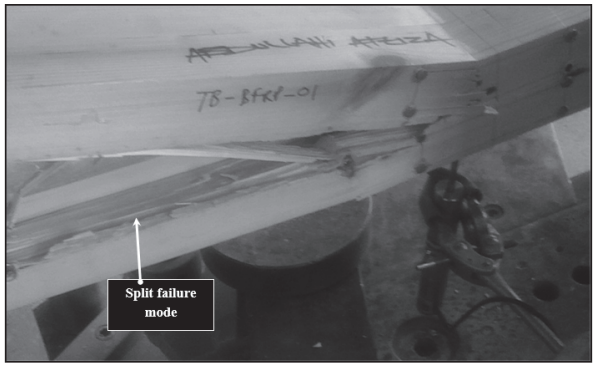

Fig. 7. Horizontal shear failure mechanism of specimen TB-BFRP-01

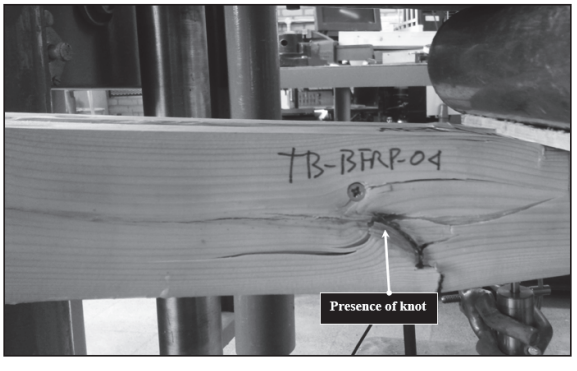

Fig. 8. Observed tensile failure of specimen TB-BFRP-04

Fig. 9. Debonded rebar following ultimate failure

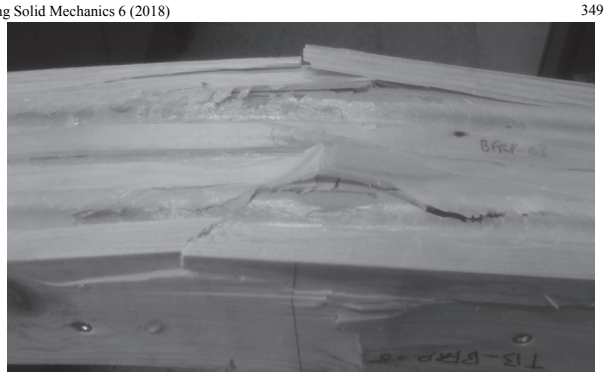

Fig. 10. Splitting at mid-span resulting in cracks in the epoxy

3.4 Load versus deflection behaviour of the timber specimen

The results for all the tested beams are shown in Figs. 11 and 12. Initially, all the beams demonstrated a linear elastic behaviour, and as the load capacity increased the graph plateaued until failure. Cracks were heard through acoustic emissions in the timber which often indicated where the non-linearity started to occur. The majority of the strengthened specimens exhibited higher ultimate load than that of the control specimens. While all the tested beams demonstrated a range of deflections of approximately 8 – 21 mm, these values do not satisfy the serviceability limit state. With reference to BS EN 1995, Eurocode 5, the deflection limit equals span/300 for a typical member between two supports. Therefore, for a beam with a clear span (L) of 1000 mm, the allowable deflection is 3.3 mm. Though a member may have a high load capacity, a low stiffness means it will not satisfy the serviceability limit state which is an essential factor.

3.5. Ultimate load capacity

The strength of the BFRP reinforced specimens generally increased in relation to the unreinforced beams. All reinforced beams exhibited an increase in load capacity except beams TB-BFRP-01 and TB-BFRP-04, from observation it is observed that these particular beams experienced severe damage such as horizontal splits, shakes and large knots located at mid-span. The ultimate load capacity, equivalent deflections and percentage differences of the unreinforced and reinforced beams are shown in Table 6. The table outlines the specimen designation, in column 1. Under this column, the reference

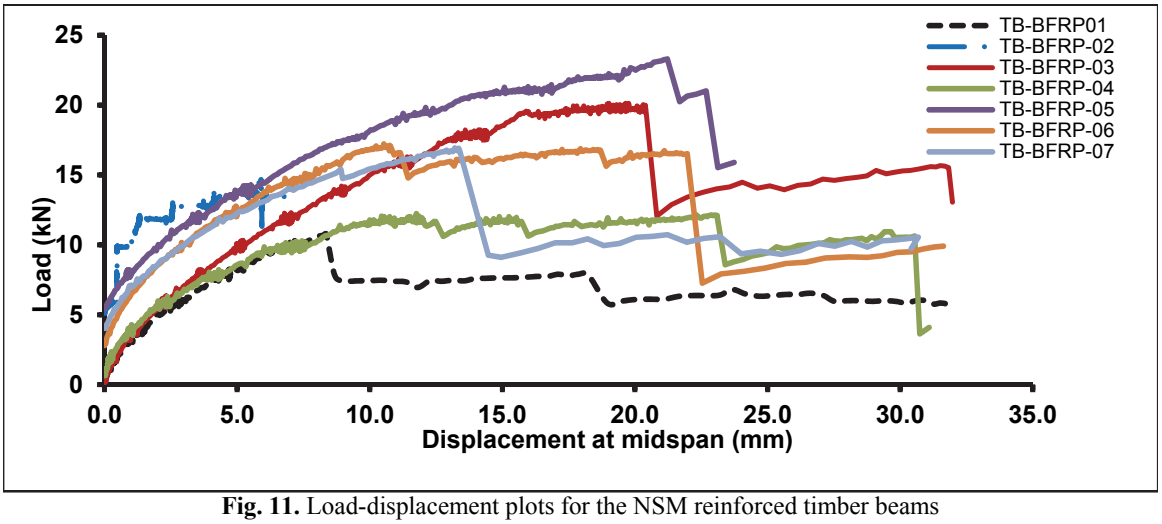

Fig. 11. Load-displacement plots for the NSM reinforced timber beams

TB-C- and TB-BFRP- denote the reference and basalt reinforced specimens, respectively. Columns 2 and 3 display the respective failure loads and mid-span displacement.

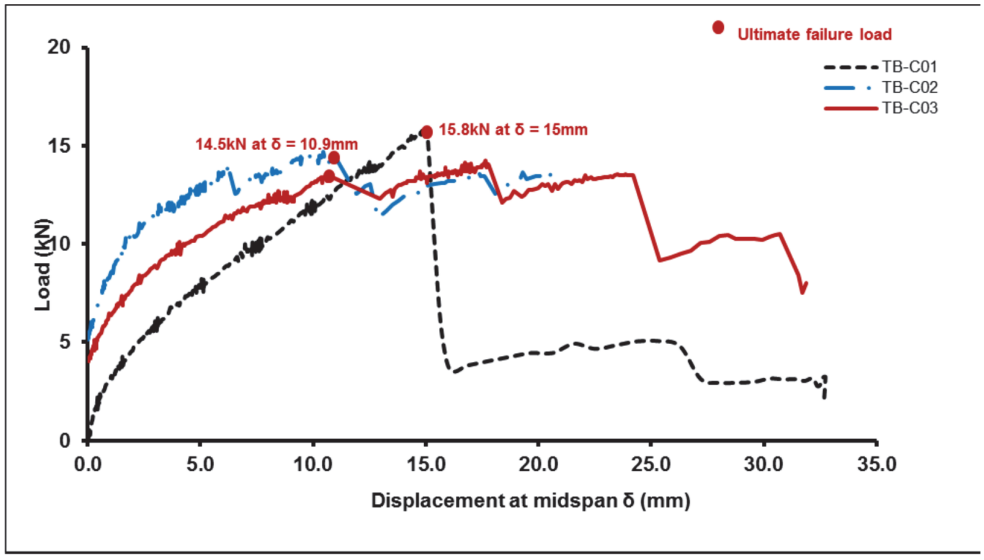

Fig. 12. Load-displacement plots for the unreinforced timber beams

Table 6. Ultimate load capacities and corresponding deflections of all test specimen

Specimen ID	Ultimate failure load, P_{ult} (kN)	Deflection at failure, δ_{ult} (mm)
TB-C-01	15.8	15.0
TB-C-02	14.5	10.9
TB-C-03	14.2	17.7
TB-BFRP-01	10.5	8.4
TB-BFRP-02	17.8	20
TB-BFRP-03	19.8	19.3
TB-BFRP-04	11.8	11.5
TB-BFRP-05	23.0	20.9
TB-BFRP-06	16.9	10.3
TB-BFRP-07	16.7	14.5

3.6 Stiffness

Initially, all beams displayed linear elastic behaviour. The behaviour of the beams was observed up until a load of 10 kN in order for the stiffness to be determined as all beams show linear relationship prior to this load. The results show that beams TB-BFRP01, TB-BFRP02, TB-BFRP03 and TB-BFRP04 were essentially less rigid when compared to the mean stiffness value of the control beams (percentage decrease ranging from 32 to 56%). When comparing beams TB-BFRP05, TB-BFRP06 and TB-BFRP07 the opposite occurs with a percentage increase ranging from 22 to 73%. Further investigations should be made to achieve more comprehensive and reliable data.

3.7 Surface strain distribution

The strain distribution was measured along the depth of the beam using demec gauges points prior to failure. The applied load was governed in a series of intervals starting from 0 kN, with an increment of 2 kN. It can be seen from control beam TB-C-01, that when the flexural compressive strain is greater than 0.5%, the compression zone begins to crush. Likewise, tension cracking occurs when the flexural tensile strain is greater than 0.5%. In comparison to control beam TB-C-01, the tensile strains of the reinforced beams typically reduced (critical strain decrease was 27%) or remained at a constant strain of approximately 0.5%. Therefore, this indicated that the BRFP had successfully reinforced the tension zone of the beams. The compressive strains of the reinforced beams were essentially greater (critical

strain increase was 60%) than that of TB-C-01 except for TB-BFRP-01 which was the only beam to clearly fail due to horizontal shearing and as a result was unable to achieve ultimate load capacity.

4. Concluding Remarks

The experimental study reported in this paper provides a further understanding of the behaviour of timber beams strengthened with NSM-BFRP rebars. A total of 10 specimens were tested under 3-point bending. The experiment included 3 unreinforced solid timber beams, and 7 BFRP reinforced beams using a near-surface mounted arrangement. The experimental data and research collected have supported the following conclusions:

1. Timber strengthened with BFRP rebar generally had an increase in its ultimate load capacity. An average percentage increase of 16% is obtained, while a maximum percentage increase of 60% was achieved.
2. The results are unclear to whether BFRP bars enhance the timbers beams stiffness. Although the stiffness of the critical reinforced and unreinforced beams presented an increase of 30%.
3. Generally, the beams failed in tension when the tensile strain was equal to or less than 0.5% while the beams failed in compression at a strain greater than 0.5%.
4. Most the BFRP rebars remained bonded to the failed timber beams. There was no sign of rupture in any of the rebar specimens after testing.
5. The control beam specimens suffered from simple and cross grain tensile failures as a result of knots (defects) located near the mid-span of the loaded timber.
6. The mode of failure was dependent on the strength of the timber, although certain beams did show signs of cracking at the adhesive glue-line.

Acknowledgement

The authors are particularly thankful to the technicians at the School of Energy, Construction and Environment, Coventry University for their assistance in the fabrication of the test specimens. Also, the authors gratefully acknowledge the support of MagmaTech Ltd., UK and Rotafix Ltd., UK, suppliers of the BFRP rebar and structural adhesive, respectively.

References

Adams, R. D. (Ed.). (2005). *Adhesive bonding: science, technology and applications*. Elsevier.

Alam, P., Ansell, M. P., & Smedley, D. (2009). Mechanical repair of timber beams fractured in flexure using bonded-in reinforcements. *Composites Part B: Engineering*, *40*(2), 95-106.

Asplund, S. O. (1949, January). Strengthening bridge slabs with grouted reinforcement. In *Journal Proceedings* (Vol. 45, No. 1, pp. 397-406).

Bank, L. C. (2006). *Composites for construction: structural design with FRP materials*. John Wiley & Sons.

Borri, A., Corradi, M., & Grazini, A. (2005). A method for flexural reinforcement of old wood beams with CFRP materials. *Composites Part B: Engineering*, *36*(2), 143-153.

Broughton, J. G., & Hutchinson, A. R. (2003). Review of relevant materials and their requirements for timber repair and restoration. *LICONS (low intrusion conservation systems for timber structures, CRAF-1999-71216, Task 2.2*.

Burgoyne, C., & Balafas, I. (2007, July). Why is FRP not a financial success. In *Proc. 8th Intl. Conf. on FRP Reinforcement for Reinforced Concrete Structures, FRPRCS-8, Univ. of Patras, Patras, Greece*.

Custodio, J., & Broughton, J. G. (2008). Factors influencing bond performance. Core Document of COST Action E34, Bonding of timber. Vienna: University of Natural Resources and Applied Life Sciences.

Davalos, J. F., Qiao, P., & Trimble, B. S. (2000). Fiber-reinforced composite and wood bonded interfaces: Part 1. Durability and shear strength. *Journal of Composites, Technology and Research*, *22*(4), 224-231.

Dempsey, D. D., & Scott, D. W. (2006). Wood members strengthened with mechanically fastened FRP strips. *Journal of Composites for Construction*, *10*(5), 392-398.

Fossetti, M., Minafò, G., & Papia, M. (2015). Flexural behaviour of glulam timber beams reinforced with FRP cords. *Construction and Building Materials*, *95*, 54-64.
Harvey, K., & Ansell, M. P. (2000). *Improved timber connections using bonded-in GFRP rods* 6th World Conference on Timber Engineering. Canada: Whistler.
Hollaway, L. C., & Teng, J. G. (Eds.). (2008). *Strengthening and rehabilitation of civil infrastructures using fibre-reinforced polymer (FRP) composites*. Elsevier.
Juvandes, L. F. P., & Barbosa, R. M. T. (2012). Bond analysis of timber structures strengthened with FRP systems. *Strain*, *48*(2), 124-135.
Li, Y. F., Tsai, M. J., Wei, T. F., & Wang, W. C. (2014). A study on wood beams strengthened by FRP composite materials. *Construction and Building Materials*, *62*, 118-125.
Micelli, F., Scialpi, V., & La Tegola, A. (2005). Flexural reinforcement of glulam timber beams and joints with carbon fiber-reinforced polymer rods. *Journal of Composites for Construction*, *9*(4), 337-347.
McConnell, E., McPolin, D., & Taylor, S. (2014). Post-tensioning of glulam timber with BFRP tendons. *Proceedings of ICE-Construction Materials*, 1-9.
Morales-Conde, M. J., Rodríguez-Liñán, C., & Rubio-de Hita, P. (2015). Bending and shear reinforcements for timber beams using GFRP plates. *Construction and Building Materials*, *96*, 461-472.
Raftery, G. M., Harte, A. M., & Rodd, P. D. (2009). Bond quality at the FRP–wood interface using wood-laminating adhesives. *International Journal of Adhesion and Adhesives*, *29*(2), 101-110.
Raftery, G. M., & Harte, A. M. (2011). Low-grade glued laminated timber reinforced with FRP plate. *Composites Part B: Engineering*, *42*(4), 724-735.
Silva, P., Cachim, P., & Juvandes, L. (2004). Técnicas avançadas de reforço de estruturas de Madeira com compósitos reforçados com fibras (FRP). In *Proceeding 1st Iberic Congress Cimad'04-Wood in Construction* (pp. 613-622).
Subramanian, N. (2010). Sustainability of RCC structures using basalt composite rebars. *The Master Builder*, *12*(9), 156-64.
Subramanian, R. V., Sundaram, V., & Patel, A. K. (1978). *Electrodeposition of Polymers of Graphite Fibers: Effects on Composite Properties* (No. TR-4). WASHINGTON STATE UNIV PULLMAN DEPT OF MATERIALS SCIENCE AND ENGINEERING.
Taylor, S., Robinson, D., & Sonebi, M. (2011). Basalt-fibre-reinforced polymer. *Concrete-Camberley*, *45*(4), 48.
Urbanski, M., Lapko, A., & Garbacz, A. (2013). Investigation on concrete beams reinforced with basalt rebars as an effective alternative of conventional R/C structures. *Procedia Engineering*, *57*, 1183-1191.
Yeboah, D., Taylor, S., McPolin, D., Gilfillan, R., & Gilbert, S. (2011). Behaviour of joints with bonded-in steel bars loaded parallel to the grain of timber elements. *Construction and Building Materials*, *25*(5), 2312-2317.
Yeboah, D., Taylor, S., McPolin, D., & Gilfillan, R. (2013). Pull-out behaviour of axially loaded Basalt Fibre Reinforced Polymer (BFRP) rods bonded perpendicular to the grain of glulam elements. *Construction and Building Materials*, *38*, 962-969.
Yusof, A., & Saleh, A. L. (2010). Flexural strengthening of timber beams using glass fibre reinforced polymer. *Electronic Journal of Structural Engineering*, *10*, 45-56.
Zhishen, W., Xin, W., & Gang, W. (2012). Advancement of structural safety and sustainability with basalt fiber reinforced polymers. *CICE2012, Rome*, *13*, 15-29.